

UDC 544.228

DOI: 10.15372/KhUR2019138

## Study on Synthesis and Densification of Non-Stoichiometric Magnesium Aluminium Spinel

J. DUAN<sup>1</sup>, X. WANG<sup>1</sup>, G. R. KARAGEDOV<sup>2</sup>, H. GAO<sup>1</sup> and J. YANG<sup>3</sup><sup>1</sup>*School of Materials Science and Engineering, Dalian Jiaotong University, Dalian (China)*

E-mail: wangxh@djtu.edu.cn

<sup>2</sup>*Institute of Solid State Chemistry and Mechanochemistry, Siberian Branch, Russian Academy of Sciences, Novosibirsk (Russia)*<sup>3</sup>*State Key Laboratory of New Ceramics and Fine Processing, School of Materials Science and Engineering, Tsinghua University, Beijing (China)*

### Abstract

MgO ·  $n$ Al<sub>2</sub>O<sub>3</sub> powder ( $n = 1, 1.25, 1.5, 1.75, 2.0, 2.5$ ) was prepared by the bimetal alkoxide hydrolysis method. The effects of changes of aluminium content on material phase, particle size, morphology, infrared transmittance, and ceramic densification were studied. The results show that the MgO ·  $n$ Al<sub>2</sub>O<sub>3</sub> ( $n \leq 2$ ) powder forms a pure phase of magnesium-aluminium spinel at 1200 °C. When  $n$  is 2.5, the characteristic peak of Al<sub>2</sub>O<sub>3</sub> appears. The particle size of powder gradually increases with an increase of  $n$  value. There were significant differences in the densification of powders with a various of magnesium/aluminium ratio. The density of samples varies greatly with the sintering temperature. When the sintering temperature is between 1200 and 1400 °C, there are no obvious changes. The density is found to be 3.45 g/cm<sup>3</sup> at the sintering temperature of 1400 °C. When  $n$  is of 1.25 and 1.5, the sample density increases with an increase of sintering temperature, reaching 3.46 g/cm<sup>3</sup> at 1550 °C. The powder with ball milling has a better sintering performance, the density of the MgO · 1.5Al<sub>2</sub>O<sub>3</sub> powder with ball milling is 3.448 g/cm<sup>3</sup> at the sintering temperature of 1600 °C, which is 2.5 % higher than that of the non-ball-milled sample at the same temperature.

**Key words:** magnesium aluminium spinel, synthesis, powder, performance

### INTRODUCTION

Magnesium-aluminium spinel has been widely studied due to its good chemical properties, high temperature resistance and mechanical properties. It has been considered as an indispensable material for infrared window, transparent armor and missile fairing in the defense industry [1–5]. Many researchers have found that Mg<sup>2+</sup> ions partly evaporate in the process of sintering magnesium-aluminium spinel transparent ceramics due to high vapor pressure at sintering temperatures, which causes a change in the stoichiometric ratio of magnesium-aluminium. Kanzaki [6]

reported the effect of non-stoichiometric ratios in magnesium-aluminium spinel ceramics on the dimensional structure and mechanical strength of ceramics. Chiang [7] studied the migration of grain boundaries of non-stoichiometric magnesium-aluminium spinel. Baudin [8] proposed the effect of stoichiometry on the fracture behavior of magnesium aluminate spinel. Many related studies on non-stoichiometric magnesium aluminate spinel have been published [9–11] since 2000. However, the research of Chinese scientists in this field is relatively late being basically started in the 1990s. Taiwanese scientists of Huang and Ting made in-depth research on the sintering of

aluminium-rich spinel ceramics [12, 13] and obtained good achievements. The literature review found that mainland scientists started very late in the research on transparent ceramics with non-stoichiometric ratio of magnesium-alumina spinel. Up to date, there are few in-depth reports on current research that are mainly focused on the preparation and physicochemical properties of sintered ceramics [14, 15], while few reports focused on aluminium-magnesium-alumina spinel powder. Herein, the aluminium-rich spinel powder with different stoichiometric ratios of magnesium and aluminium was synthesized by a bimetal alkoxide hydrolysis process, and its properties were studied.

## EXPERIMENT

### Chemicals

Mg foil (99.9 %) and Al foil (99.9 %) were obtained from Tianjin Bodi Chemical Co., Ltd., urea (AR), alcohol (AR), isopropanol (AR) were purchased from Shanghai Reagents Factory. The deionized water was directly made in the experiment.

### Preparation of magnesium-aluminium spinel

Mg and Al foils were first ground and cleaned with ethanol. The treated Mg and Al were weighed to obtain certain molar ratio and then added into the reaction kettle with an excess of isopropanol.

Having been heated at 85 °C under reflux conditions, the resulting  $\text{MgAl}_2(\text{OC}_3\text{H}_7)_8$  was distilled off. Certain amounts of urea, isopropanol and deionized water were added at 20 °C to form hydrolyzate. The hydrolyzate was dried at 80 °C for 4 h, then placed in a muffle furnace and calcined at 1200 °C for 2 h. The ratio of magnesium and aluminium was adjusted to prepare powder of  $\text{MgO} \cdot n\text{Al}_2\text{O}_3$  ( $n = 1.25, 1.5, 1.75, 2.0, 2.5$ ).

Magnesium aluminium spinel powder and alumina 5 mm grinding balls were put into a grinding tank based on the proportion of mass ratio of 1 : 10. Alcohol was used as the grinding medium and a low-speed grinding was conducted for 3–8 h. The resulting powder was dried under 110 °C for 24 h, and sieved (pore diameter of 75  $\mu\text{m}$ ), followed by compaction into a circular tablet with a diameter of 2 cm and thickness of 0.5 cm by pressing. The circular tablet was sintered at 1300–1650 °C. The heating rate was of 5 °C/min, and the holding time was 3 h.

### Characterization

The X-ray diffraction (XRD) of samples was measured by an X-ray diffractometer (D/max-3B type, Nippon Ryokan Co., Ltd.). The morphology of the powder was observed by a scanning electron microscope (SEM, JSM-6360LV, JEOL Co., Ltd.). The particle size and particle size distribution of the powder were tested by a laser particle size analyzer (Mastersizer 2000, UK Malvern). The density was measured by the Archimedes drainage method with the accuracy  $\pm 0.001 \text{ g/cm}^3$  [16]. The infrared transmittance of the sample was determined by a Fourier transform infrared-Raman spectroscopy. During the sample treatment, 150 mg of KBr solids were mixed with 1 mg of the sample and subjected to compression molding using a hydraulic tableting machine.

## RESULTS AND DISCUSSION

### Analysis of XRD and Infrared results of different samples

The XRD patterns of powders annealed at 1200 °C are presented in Fig. 1, *a*, the diffraction peaks assigned to crystal plane (440) of  $\text{MgO} \cdot n\text{Al}_2\text{O}_3$  being demonstrated on Fig. 1, *b*. Figure 1, *a* shows that the powder has a good crystallinity, and when parameter  $n$  is within 1.5–2.0, the respective diffraction peaks and relative intensities of the corresponding powder materials are consistent with the ones in the standard card of magnesium-aluminium spinel. It indicates that the excess of Al ions is completely integrated into the  $\text{MgAl}_2\text{O}_4$  spinel structure, and the powders are pure phase magnesium-aluminium the spinel structures. When parameter  $n$  equals to 2.5, apart from characteristic peaks of the spinel structure, peaks attributed to crystal planes of (012), (104) and (113) of  $\text{Al}_2\text{O}_3$  appear in the pattern. It indicates that  $\text{MgAl}_2\text{O}_4$  phase and  $\alpha\text{-Al}_2\text{O}_3$  phase are simultaneously present in the powder.

The diffraction peak in Fig. 1, *b* shifts toward a large angle with increasing content of aluminium. Owing to the availability of a large number of empty tetrahedral and octahedral sites, the unit cell of  $\text{MgAl}_2\text{O}_4$  is considered as a host cell capable of holding a large number of trivalent cations in solid solution. According to the phase diagram [17] solid solutions containing a lot of excess of  $\text{Al}^{3+}$  ions really exist at high temperatures. Our powders may well be thermodynamically metastable and taking into account that Al–O bond is shorter than that of Mg–O in spinel structure one

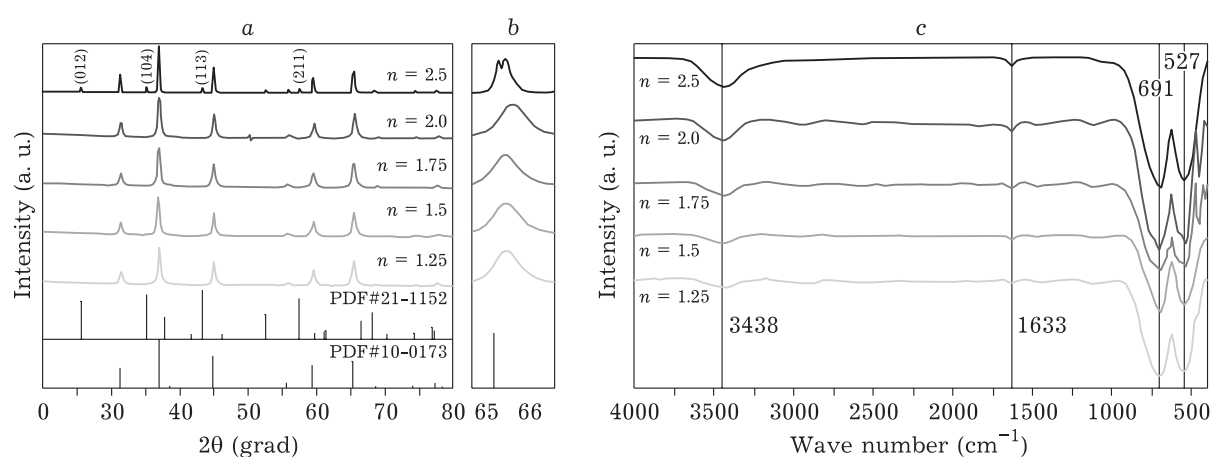


Fig. 1 XRD patterns (a), diffraction peaks at crystal plane (440) (b) and IR transmission spectra of  $\text{MgO} \cdot n\text{Al}_2\text{O}_3$  powder (c), ( $n = 2.5$  (1); 2.0 (2); 1.75 (3); 1.5 (4); 1.25 (5)).

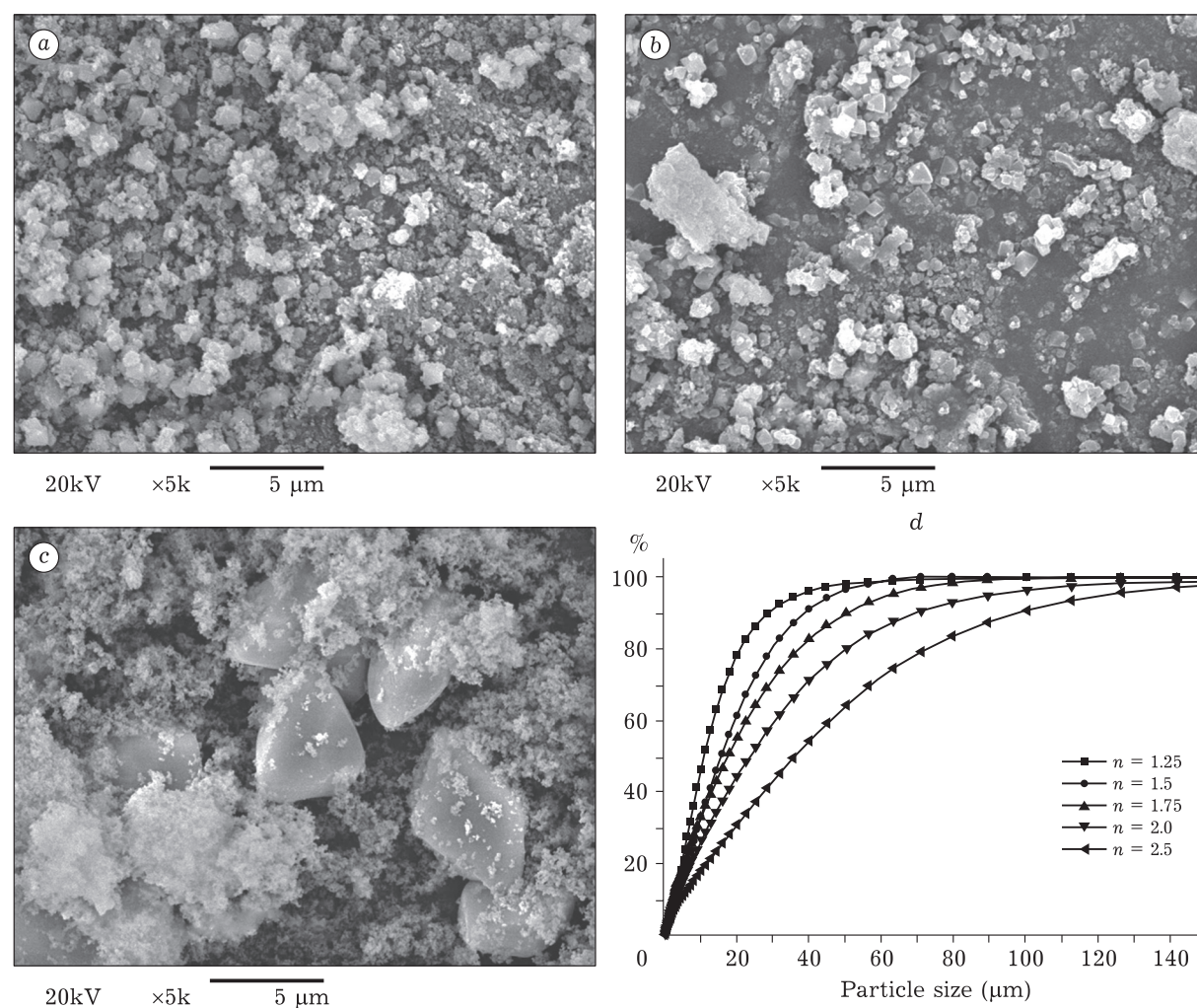


Fig. 2. SEM images of sample  $\text{MgO} \cdot n\text{Al}_2\text{O}_3$ ;  $n = 1.25$  (a);  $n = 1.75$  (b);  $n = 2.5$  (c) and percentage of particles with the diameter below the value on X-axis (d).

comes to the conclusion that lattice parameter of the solid solution should be less and cause the shift of the diffraction peaks.

Figure 1, *c* is IR transmission spectra of the powders. There are obvious hydroxyl absorption peaks as the band of  $3438\text{ cm}^{-1}$  (hydroxyl stretching vibration peak) and  $1633\text{ cm}^{-1}$  (bending vibration peak of hydroxyl group), respectively. As the Al content increases, the intensity of the absorption peak is significantly improved. The absorption peak of the sample at a wave number of  $691\text{ cm}^{-1}$  was ascribed to a weak absorption peak of  $\text{CO}_3^{2-}$ , mainly caused by the reaction of  $\text{CO}_2$  adsorbed on the surface with water to generate  $\text{CO}_3^{2-}$ . The absorption peak of the sample at a wave number of  $527\text{ cm}^{-1}$  can be attributed to the characteristic peak of  $\text{AlO}_4^{2-}$ .

#### Analysis of morphology and size of different sample

Figure 2, *a–c* shows the SEM images of  $\text{MgO} \cdot n\text{Al}_2\text{O}_3$  ( $n = 1.25, 1.75, 2.5$ ). When  $n$  equals 1.25 the particle size of the powder is small. As the value of  $n$  increases, the particle size of the powder gradually increases. The main reason is that when the value of  $n$  is small, the rate of nucleation is large, and a large number of primary particles are generated. As the value of  $n$  increases, the growth rate of the nucleus is larger than the rate of the nucleation, resulting in the introduction of particles. The diameter starts to increase. This is mainly because the aluminium-rich spinel is a defect-type solid solution, and  $\text{Mg}^{2+} \rightarrow \text{Al}^{3+}$  non-equivalent substitution occurs, resulting in a smaller lattice spacing, a larger bulk density, and a

denser material, which can effectively reduce the thermal diffusivity.

Comparing the curves in Fig. 2, *d*, it can be seen that as the value of  $n$  increases, the particle size of the powder gradually increases, and the particle size distribution tends to be wide.

#### Effect of different magnesium-aluminium ratios on densification of ceramics

The density of the sample increases obviously with the increase of the sintering temperature in Fig. 3, *a*, and the change trend is related to the magnesium-aluminium ratio. When the molar ratio of Mg/Al is 1 : 2, the sintering temperature is raised from 1200 to 1400 °C, the sample density greatly changes. When the sintering temperature is higher than 1400 °C, no more significant changes in the density were observed with the sintering temperature, and the density is  $3.45\text{ g/cm}^3$  at 1400 °C. When the molar ratio of Mg/Al is (1 : 2.5)–(1 : 3.0), the density of the sample increases with the increase of the sintering temperature, reaching  $3.46\text{ g/cm}^3$  at 1550 °C. As the Al content continues to increase, with a molar ratio of Mg/Al as 1 : 3.5, the sample density increases with an increase of sintering temperature below 1400 °C. Slight changes in the density are detected when the sintering temperature continues to increase. The main reason is that the temperature of forming the spinel phase is different for samples with various ratios of magnesium-aluminium. Compared with  $\text{MgAl}_2\text{O}_4$ , the temperature of forming the spinel structure is relatively high for the excess Al sample, which leads to the

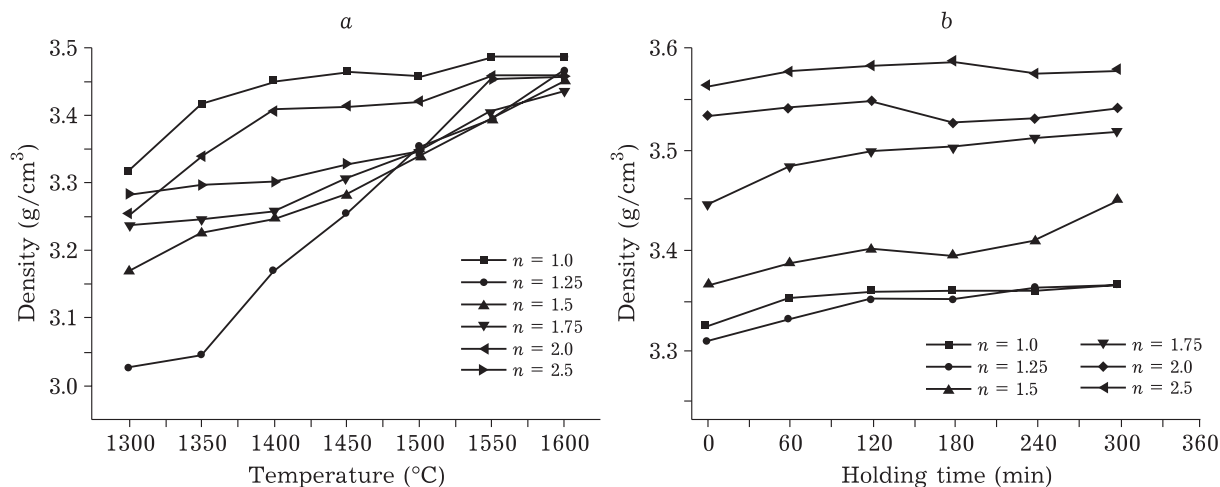


Fig. 3. Curve of the density change with the sintering temperature (*a*) and with holding time sintered at 1400 °C (*b*) of  $\text{MgO} \cdot n\text{Al}_2\text{O}_3$ .



simultaneous phase reaction and sintering densification. Therefore, the final sample depends on the relative contributions of the two. When the Mg/Al ratio is larger than 1 : 2.5, the magnesium-aluminium spinel phase can be formed at a lower temperature, and a small amount of  $\text{Al}_2\text{O}_3$  remaining inside the sample is solid-solved when the sintering temperature continues to rise, and the volume expansion is very small, so densification dominates throughout the sintering process, and the density of the sample increases as the sintering temperature increases. When the Mg/Al ratio is less than 1 : 3.0, the formation temperature of the magnesium-aluminium spinel phase is obviously increased. There is a large amount of  $\text{Al}_2\text{O}_3$  in the sintering densification process.  $\text{Al}_2\text{O}_3$  begins to solidify into the crystal lattice at the formation temperature of the spinel phase. This process causes the sample to shrink in volume and offsets the volume expansion of the lattice formation, so the density of the sample does not change and may even decrease.

Figure 3, b shows the curve of density changing with the holding time at 1400 °C. When the molar ratio of Mg/Al is 1 : 2.5 or even less of Al, the density of the sample increases with the extension of the holding time. The sample density basically did not change after holding for 1 h. But when the aluminium content increased with the exceeds molar ratio of Mg/Al 1 : 3.0, the density showed small fluctuations. It indicates that the densification of samples with magnesium-aluminium ratios is affected by the factor of holding time.

#### *Effect of powder particle size on ceramic densification*

The particle size and surface area of  $\text{MgO} \cdot 1.5\text{Al}_2\text{O}_3$  samples are listed in Table 1 and Fig. 4, a.

The  $D_{50}$  (cumulative mass percent finer) of the powder was reduced from 17.67 to 4.81  $\mu\text{m}$  with ball milling for 6 h, while the specific surface area increased from 0.97 to 4.36  $\text{m}^2/\text{g}$  the particle size distribution of powder with ball milling is narrower compared to that of powders with no ball milling.

TABLE 1  
Particle size and specific surface area data of  $\text{MgO} \cdot 1.5\text{Al}_2\text{O}_3$  powder

Treatment of sample	$D_{10}$ ( $\mu\text{m}$ )	$D_{50}$ ( $\mu\text{m}$ )	$D_{90}$ ( $\mu\text{m}$ )	Specific surface area ( $\text{m}^2/\text{g}$ )
Non-ball milling	3.664	17.672	42.854	0.97
Ball milling	2.063	4.806	12.838	4.36

Figure 4, b shows the relationship between the density of the sample after sintering. The density of the sintered samples increases rapidly from 1450 to 1550 °C, and the density of the sintered samples with no ball milling and ball milled sample increases from 2.924 to 3.339  $\text{g}/\text{cm}^3$  and from 3.108 to 3.385  $\text{g}/\text{cm}^3$ , respectively. The density of the sintered sample with ball milling is 3.448  $\text{g}/\text{cm}^3$  at 1600 °C, and 2.5 % higher than that of the sample with no ball milling. The density of the sample with ball milling is always higher than that of the sample with no ball milling, which is mainly due to the synthesis process on the powder. When the powder is synthesized by bimetallic alkoxide hydrolysis, agglomeration will inevitably occur in the hydrolysis process, resulting in the presence of agglomerates in the powder, leading to a wide particle size distribution. However, the aggregates in the powder material can be eliminated by ball milling, which not only refines the powder particles but also reduces the particle size distribution range. It is beneficial to the compactness of powder sintering.

Figure 4, c–h displays the SEM images of samples calcined at different temperatures. It can be seen that the sample is not sintered at 1400 °C, and the large particles are distinct. The samples show a certain degree of sintering at 1500 °C. When the calcination temperature is increased to 1600 °C, the density of the samples is significantly improved after ball milling. Compared to the sample with non-ball milling, the sample with ball milling has less obvious pores and smaller pore size, resulting in a relatively higher density.

#### **CONCLUSION**

The aluminium-rich spinel ( $\text{MgO} \cdot n\text{Al}_2\text{O}_3$ ) powders were successfully prepared by the bimetal alkoxide hydrolysis method and effect of magnesium-aluminium ratio on densification of samples during high temperature was investigated. The conclusions are as follows.

1. When  $n < 2.5$ , the pure phase of magnesium-aluminium spinel structure is obtained at 1200 °C,

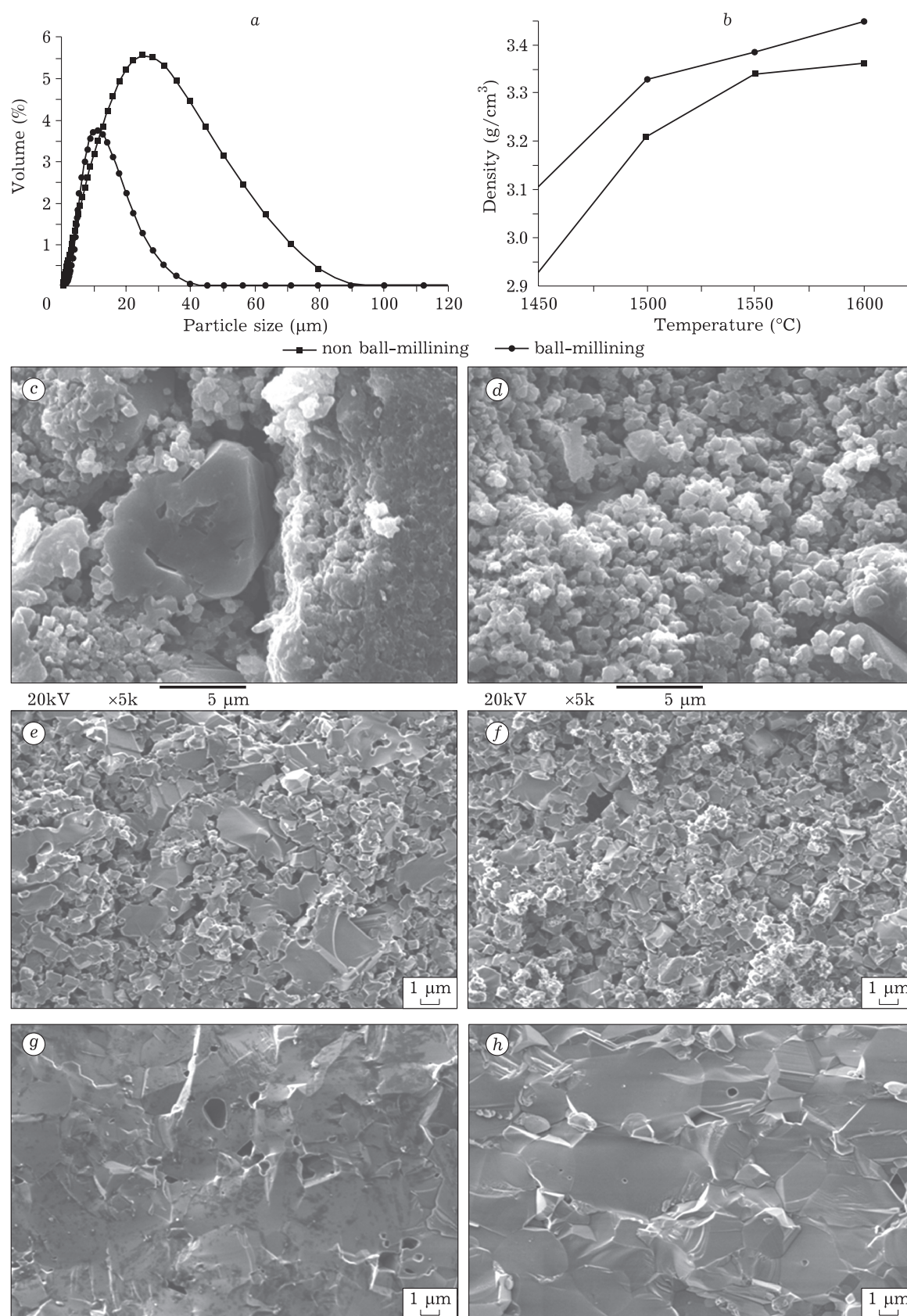


Fig. 4. Particle size distribution of  $\text{MgO} \cdot 1.5\text{Al}_2\text{O}_3$  powder sintered at 1200 °C (a) and relationship between density and sintering temperature of  $\text{MgO} \cdot 1.5\text{Al}_2\text{O}_3$  sintered samples, holding for 3 h (b) and SEM image of the sample at different calcination temperatures: (c) non ball milling, 1400 °C; (d) ball milling, 1400 °C; (e) non ball milling, 1500 °C; (f) ball milling, 1500 °C; (g) non ball milling, 1600 °C and (h) ball milling, 1600 °C.

and as the value of  $n$  increases, the diffraction peak shifts to a large angle.

2. The higher the Al content is, the higher the temperature is required for densification.

3. Ball milling can improve the sintering properties of powders. The density of the sample  $\text{MgO} \cdot 1.5\text{Al}_2\text{O}_3$  is  $3.448 \text{ g/cm}^3$  with ball milling at  $1600^\circ\text{C}$ , which is 2.5 % higher than that of the without ball milling.

## REFERENCES

- 1 Marc R. M., Hans-Joachim K. // J. Am. Ceram. Soc. 2013. Vol. 96, No. 11. P. 3347.
- 2 Wang S. F., Zhang J. // Prog. Solid State Ch. 2013. Vol. 41. P. 40.
- 3 Ganesh I. // Inter. Mat. Rev., 2013. Vol. 58, No. 2. P. 63.
- 4 Yu H. Z. // Infrared Optical Materials. Beijing: National Defense Industry Press, 2015.
- 5 Gamesh I., Srinivas B. // Bull. Ceram. Trans. 2002. Vol. 101. P. 247.
- 6 Kanzaki S., Nakagawa Z. E. // J. Ceram. Assoc. Jpn. 1979. Vol. 87, No. 5 P. 230.
- 7 Chiang Y. M., Kingery W. D. // J. Am. Ceram. Soc. 1989. Vol. 72, No. 2. P. 271.
- 8 Baudin C., Pena P. // J. Eur. Ceram. Soc. 1997. Vol. 17. P. 1501
- 9 Robert I. S., Thomas H. // J. Am. Ceram. Soc. 1999. Vol. 82, No. 12. P. 3293.
- 10 Sutorik A. C., Gary G. // J. Am. Ceram. Soc., 2012. Vol. 95, No. 6. P. 1807.
- 11 Waetzig K., Krell A. // J. Am. Ceram. Soc. 2016. Vol. 99, No. 3. P. 946.
- 12 Huang J. L., Sun S. Y. // Mater Sic Eng. A. 1999. Vol. 259, No. 1. P. 1.
- 13 Ting C. J., Lu H. Y. // J. Am. Ceram. Soc. 2000. Vol. 83, No. 7. P. 1592.
- 14 Li W., Lei M. Y. // Bull. Chin. Ceram. Soc. 2011. Vol. 30, No. 4. P. 851.
- 15 Huang C. B., Wei C. L. // Bull. Chin. Ceram. Soc., 2010. Vol. 29, No. 2. P. 464.
- 16 Tian S., Wang W. M. // Physical Testing and Chemical Analysis. Part A: Physical Testing. 2011. Vol. 47, No. 8. P. 476.
- 17 Hallstedt B. // J. Am. Ceram. Soc. 1992. Vol. 75. No. 6. P. 1497–1507.

